FLUID-MINERAL EQUILIBRIA OF FLUIDS FROM PRODUCTION WELLS OF THE SANDAWA SECTOR, Mt. APO, PHILIPPINES

Benson Ma. Sambrano

PNOC-Energy Development Corporation, Fort Bonifacio, Makati City, Philippines

Abstract

The Mindanao 1 geothermal field is located on the northwestern flanks of Mt. Apo, Cotabato province in the island of Mindanao, Philippines. Four of the wells drilled in the Sandawa Collapse will be producing for the second stage development of a 52 MWe power plant. The scope of this study is to assess water and gas compositions from the Sandawa production wells and to interpret the results in relation to the reservoir conditions and fluid mineral equilibria.

The evaluation of water compositions from the Sandawa production wells show that there are two types of fluids discharged, the near neutral to neutral pH chloride water and the mixed chloride sulfate water. The Cl-waters comprise the fluids residing at reservoir depths which have a Cl content of ~6600 mg/kg. The equilibration temperature based on the Na-K-Mg geothermometer at the reservoir is 320°C which is in accordance with the measured downhole temperatures.

Evaluation of gas compositions indicate that the fluids have undergone continuous degassing from deeper horizons to the present reservoir depths tapped by the wells. The degassing is presently occurring as shown by the two-phase conditions exhibited by the well discharges. The degassed characteristics of the fluids are reflected in gas equilibration, resulting in vapor losses in TM-1, TM-2 and KN-3 to as much as 5 percent. The gases are assessed to be unequilibrated based on the CO_2/Ar and H_2/Ar ratios. Gas geothermometers predicted a variable range of temperatures from 210-321°C, however, the temperatures estimated by carbon dioxide-argon geothermometer closely agree with measured downhole temperatures.

Aqueous speciation calculations using the computer program WATCH shows that the fluids from the wells (TM-1, TM-2, KN-3) are saturated with respect to anhydrite and undersaturated with calcite at reservoir conditions. With respect to the cationic components, the fluids are found to be primarily in equilibrium with K-mica at the reservoir, however, the fluids approaching TM-2 conditions are also in equilibrium with albite, wairakite, K-feldspar and calcite. Owing to the low CO_2 content of the fluids, other calc-silicates may form readily. Hydrothermal alteration mineralogy from these wells indicate wairakite, adularia and calcite are found to exist in the rocks at the reservoir. Moreover, sulfide reactions do not influence hydrogen-hydrogen sulfide equilibria but arise as a result of the redox state of the fluids. This results in the stability of pyrite plus other sulfides in the system.

Introduction

1. Background

The Mindanao 1 Geothermal Production Field is one of the operating fields of the PNOC-Energy Development Corporation. The field is situated on the northwestern flanks of Mt. Apo, Cotabato province in the island of Mindanao (Figure 1). Surface exploration began in 1983 and ascertained the existence of a potential energy resource with a 15-28 km^2 geophysical anomaly. Deep exploratory drilling was then conducted in 1987-1988 which established the high temperature resource of the area. Subsequent drilling in 1992 provided more information on the geothermal system, which led to the development of the area. There are 26 wells drilled in the field to date. At present, **Mindanao 1** Geothermal field is operating a 52 MWe power plant which was commissioned in March 1997. production for the power plant draws from nine wells located in the Marbel sector. A second stage development for another 52 MWe power plant is underway with planned production from wells of the Sandawa sector.

2. Previous Work

Delfin, et al.(1984) presented the surface exploration data conducted in 1983 whch consisted of the detailed surface geology of the area, the chemical and physical characteristics of the thermal features and the resistivity survey results. Subsurface petrological data from cores arid cuttings analyses of the earliest two deep wells were presented by Reyes (1988). A minimum of 290 MWe power potential was suggested in a preliminary resource assessment (PNOC-EDC, 1989). Subsequent petrological and geochemical data from the development drilling and well testing in 1992 onwards are documented in PNOC reports held in the PNOC-EDC geothermal library. By 1994, a resource evaluation update was prepared by the geoscientific staff which reviewed the geochemical database integrating additional information from discharge tests of newly drilled wells. Isotope studies were conducted then to supplement the existing understanding of the geothermal system. Monitoring and studies continue to be conducted by the geoscientific group.

3. Scope of Study

Present energy production for the second stage 52 MWe power plant is expected to produce from wells

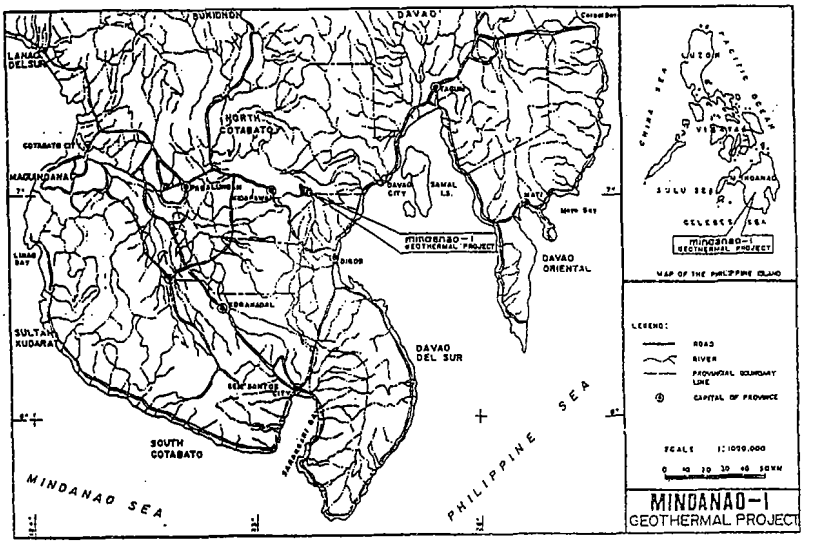

Figure 1. Location Map of the Mindanao I Geothermal field, Mt. Apo, Philippines (PNOC-EDC 1994)

drilled in the Sandawa sector of the geothermal field. The 1994 resource assessment discussed in detail the conceptual model of the Mt. Apo system with information from discharge tests of wells drilled in this sector. The scope of this study is to assess water and gas compositions from the Sandawa production wells and interpret results in relation to reservoir conditions. This report begins with an overview of the Mt. Apo geothermal system in terms of the geological and hydrological setting of the area. The geothermal wells are described along with the subsurface alteration found in these wells. In the second part, the various aspects of water and gas chemistry is assessed to define the Mt. Apo system. A selection of geochemical "tools" in assessing fluid chemistry are used to establish the reservoir conditions. These includes the tedious but powerful chemical speciation calculations using the program WATCH. The production wells TM-1, TM-2, TM-3 and KN-3 are the focus of this study. A review of the geochemical database from the medium term discharge tests conducted in 1994, 1995 and 1996 is undertaken in order to narrow the data set studied.

This study is basically limited to the four production wells of the Sandawa sector. This report does not encompass the larger aspect of the geochemical structure of the Mt. Apo system, and instead deals mainly with what the thermal waters say about the reservoir in relation to fluid-mineral equilibria.

The Mt. Apo Geothermal Field

1. Geological Setting

The Mt. Apo geothermal field is located at southwest central part of the island of Mindanao, Philippines. The main field is situated at the northwestern flanks of Mt. Apo about 40 aerial kilometers west of Davao City (Figure 1). Regional stratigraphy and tectonic studies conducted by Delfin, et *al.* (1989) indicate the system to be of Pliocene-Quaternary age and forms part of three large coalescing strato-volcanoes that transect the central region of Mindanao. Deep exploratory and development drilling established the subsurface geology of the area (Reyes, 1988; Zaide-Delfin, 1993; Maturgo and Zaide-Delfin, 1993; Panem and Zaide-Delfin, 1993; Maturgo and Rossel, 1993; Camit, 1994; Sambrano, 1994; Panem, 1995). Figure 2 shows the geological setting of Mt. Apo, and it includes the location of thermal features found to the northwest and southeast along the main tectonic grain.

The geothermal system is dominated by rocks belonging to the Apo Volcanics (AV). The young AV found mostly to the east and south of the summit is composed of andesitic domes and lavas. The older AV (AV1) is distributed dominantly to the northwest and western side of the main system. The rock formation is subdivided into two subunits namely, the Upper (older) Apo Volcanics and the Lower (older) Apo Volcanics, which are separated by a hematized claystone. The upper member is composed of hornblende andesite, dacite and minor pyroxene basaltic andesite lavas, tuff breccias and hyaloclastites. Basaltic andesite to basalt and minor pyroxene andesite lavas, tuff breccias and hyaloclastites comprise the lower member. An underlying sedimentary unit was encountered in one well, APO-2D, which was drilled to the north. The deeper horizons close to the southeast central of the system show a completely altered zone believed to be the metamorphic contact aureole of the Sandawa Intrusive (Camit, 1994).

Structural control of the Mt. Apo system is characterized by a dominant northwest-southeast trending fault system. Figure 2 shows the main structural features of the field. To the northwest is a system of steeply dipping, curvilinear faults known as the Matingao block The northwest-southeast trending Marbel fault zone adjoins the sector known as the Sandawa Collapse to the southeast. Crosscutting faults in the N-S and NE direction dissect the major faults. Some thermal features are located within the 12 km^2 diameter collapse structure such as steam vents found in the northern rim, acid sulfate and sulfate bicarbonate springs. A third of the area is underlain by acid altered ground produced through rock leaching by acid sulfate waters at shallow depths.

The overall permeability is controlled by the steeply dipping faults. The northwest-southeast trending faults appear to exhibit the highest permeabilities based on drilled zones, e.g. Sabpangon South and the Marbel fault zone. The Sandawa Collapse did not show permeability when it was intersected by wells TM-1, TM-2, TO-1 and TO-2. It appears to form a barrier for upflowing fluids and redirects flow through the Marbel fault zone.

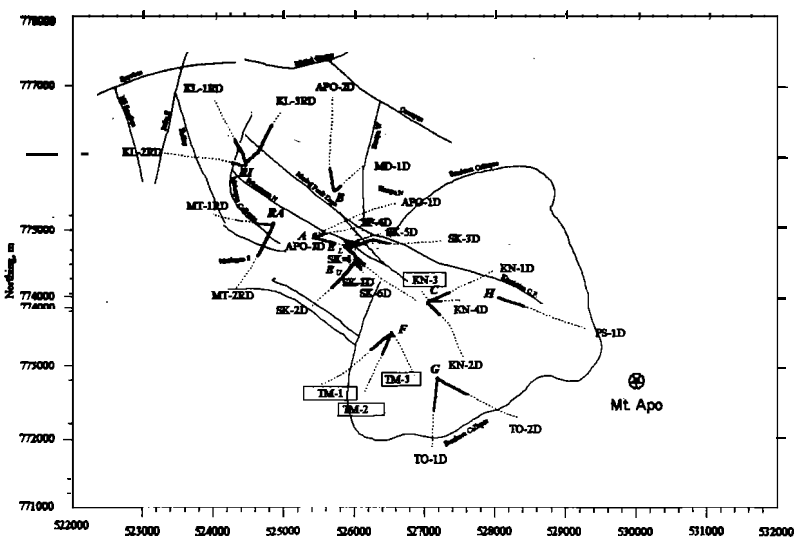

drilling intersects

2. The Geothermal Wells

Figure 2 shows the location and welltrack configuration of the 25 wells drilled in the Mt. Apo geothermal field Nine wells have been tapped for production of the first 52 MWe power plant. These wells are located in well pads (A, E_{upper} and E_{lower}) in the sector named Marbel Comdor. The wells draw fluids from the reservoir with temperatures of 250-260°C. Five reinjection wells were drilled for waste water disposal at the Matingao and Kullay block at the northwest area of the field (pad RA and RI). Ten wells were drilled in the Sandawa Collapse originating from different well pads namely, C, F, G and H. However, only four wells are considered for production in the second phase development from this sector namely, TM-1, TM-2, TM-3 and KN-3. Measured reservoir temperatures at this sector reach 300°C.

Well KN-3 is the deepest well drilled in the central sector of the Sandawa Collapse. The well was spudded from pad C at an elevation of 1698 masl. It has a total vertical depth of 2928 m (-1230 mrsl) at a throw of 192 m to the northwest. The well was cased up to 1235 m (462 masl). The hottest temperature measured in the well is 324°C at -1200 mrsl (M.B. Esberto, pers. commun., 1997). Petrologic data predicted temperatures in excess of 300°C, showing close agreement with the measured temperature. Apart from drilling through the altered Apo Volcanics, the well penetrated an intrusive body whch consists of a relatively fresh biotite hornblende quartz monzodiorite at 2480 m (-782 mrsl) down to total depth drilled (Camit, 1994). The well discharged slightly acidic fluids at pH = 5. Cyclic characteristics in its Qscharge indicated two-phase reservoir conditions believed to be dominated by a feedpoint in the upper section of the well near the production casing shoe (–500 mrsl). However, subsequent discharge tests indicated the main feed is located at the bottom of the well.

Wells TM-1, TM-2 and TM-3 were spudded from pad F, half a kilometer southwest of pad C, at an elevation of 1830 masl. These wells penetrated the Apo Volcanics from surface down to the respective target depths.

Well TM-1 was drilled with a deviation to the southwest and reached a bottomhole depth of 2087 m (-257 mrsl) and a throw of 1232 m. The well was cased to a depth of 910 m (920 mrsl). Measured tempemtures in the well indicated a maximum of 279°C at 2036 m (-206 mrsl) which coincided with the

predicted temperature based on mineral geothermometry (Rosell, 1994; Sambrano, 1994). The well discharged neutral pH fluids when it was tested in December, 1994 to January, 1995. The well is primarily fed by fluids entering a permeable zone at 1954 m (-124 mrsl) associated with a fault structure. Minor permeable zones are also indicated at shallower depths associated with other fault intersects.

Well TM-2 was targetted towards the southwest and reached a total depth of a 1822 m (6 masl) and a throw of 923 m. The production casing shoe was set at 987 m (843 mrsl). Temperature measurements conducted on the well indicated a maximum temperature of 272°C. Mineral geothermometry predicted temperatures >290°C (Rosell, 1994; Sambrano, 1994). Mineral assemblage indicate neutral pH alteration from surface down to the bottomhole. A thin zone of possibly active acid zone was found at 1742 m (88 masl) characterized by an assemblage of diaspore + pyrophyllite + alunite + pyrite ± chalcopyrite. Permeability is associated with a fault at 1753 m (77 masl). The well discharged neutral pH fluids during its medium term testing conducted February to May 1995.
Well TM-3 was drilled towards the southeast to a total depth of 1743 m (87 masl) and a throw of 715 m. The well encountered total loss of circulation at a depth of 1025 m (805 masl). The production casing shoe was set at 895 m (935 masl). Measured temperatures indicated 270°C which agree with the predicted temperatures based on mineral geothermometry. Pernieablity is associated with the total loss of circulation at 1025 m. The well discharged about 90% steam during its testing.

3. Subsurface Alteration

The alteration mineralogy exhibited by the cores and cuttings from the wells drilled within the Sandawa Collapse consists of primarily of quartz + illite + chlorite + epidote + actinolite + secondary biotite ± wairakite ± adularia which is a neutral pH assemblage except for PS-1 (Camit, 1994; Maturgo, 1994; Rosell, 1994; Sambrano, 1994). Temperature dependent mineralogy composed dominantly of illite + epidote + actinolite + secondary biotite denote progradational temperatures with respect to depth which reach 300°C at greater than 1600 m below the surface (– 100 masl). The thermal range of mineral stabilities coincide with measured temperatures downhole. Fluid inclusion data likewise indicate homogenization temperatures of 300°C.

The vertical zonation of clay minerals smectite-illite, illite-smectite and illite, reflect progressive temperature with respect to depth. Epidote first occurrences are used to denote temperatures >220°C found at 800-1000 masl. Increasing abundance and crystallization of epidote signify temperatures >260°C found at depths between 400-700 masl. At greater than 1600 m (–100 masl), actinolite and secondary biotite dominate the alteration indicating >280°C encountered by wells drilled at the central section of the Sandawa Collapse (e.g. KN-3).

Carbonates are minor in this along with wairakite Occurrences encountered in wells TM-1, TM-2, KN-1 and KN-3 indicate low CO_2 contents in the reservoir liquid (e.g. Browne and Ellis, 1970).

Cold inflow indicators such as hematite and goethite are confined to shallow depths in all the wells drilled in Sandawa Collapse. Minor zones of cold inflow were also noted to penetrate deep but occur only as discrete horizons.

Sulfides composed of bornite + chalcopyrite + pyrite were found in wells KN-1, KN-2 and KN-3. Pyrite persists in weak to moderate amounts in deeper horizons. Active acid alteration was encountered in wells PS-1 and TO-1 where the assemblage diaspore + alunite + pyrophyllite existed along with anhydrite + pyrite ± chalcopyrite (Maturgo and Zaide-Delfin, 1993; Rosell, 1994, 1995). Acid alteration in other wells consisted of rare, near-surface alunite and minor amounts of relict diaspore ± pyrophyllite. Variations in the water level are also indicated by the presence of relict epidote at shallow zones where it is altered to clay. Vapor inclusions in anhydrite and calcite crystals indicate two-phase zone existed at depth.

4. Hydrological Model

Temperatures in excess of 300°C are indicated within the Sandawa Collapse. Fluids are upwelling from this sector of the field and migrate northwest along a series of faults making up the Marbel Corridor. Based on the well discharges, the chloride content of the parent fluid is 6600 mg/kg. The fluids boil as it ascends forming steam that accumulates at the upper horizons of the reservoir. Lateral movement of the fluids leads to mixing and dilution by cold meteoric waters resulting in the decrease of chloride content and temperature. Temperature reversals at depth characterize fluid outflow path in systems of high relief These are found in wells drilled outside the Sandawa Collapse. Deep recharge is believed to occur from west of the Matingao block. Figure 3 illustrates the idealized hydrological model of the Mt. Apo geothermal system.

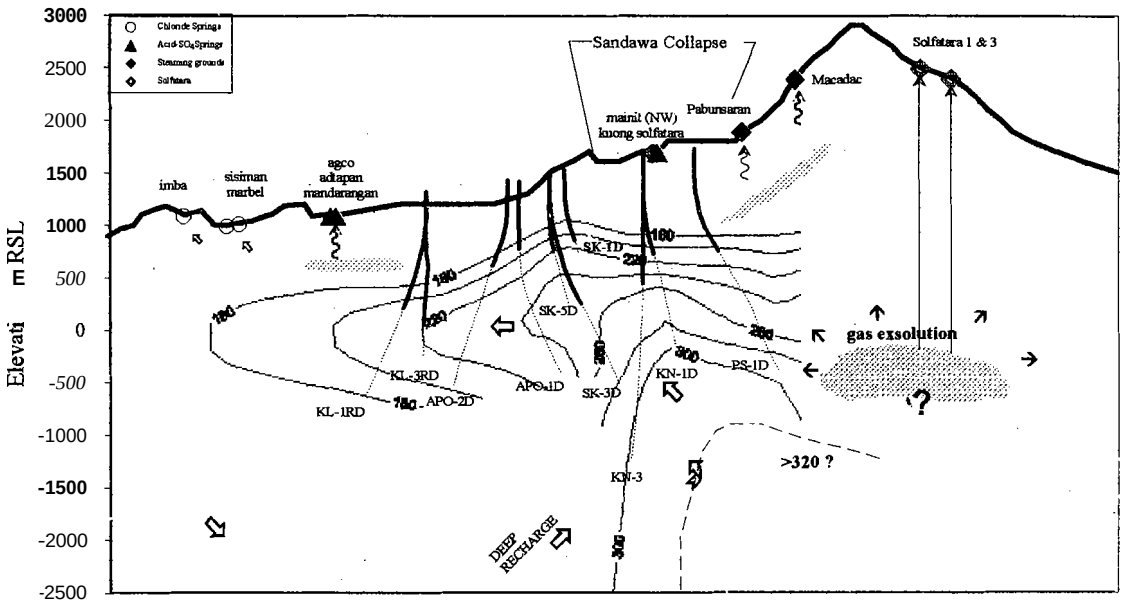

Figure 3. The idealized hydrological model of Mt. Apo geothermal system (modified from Salonga, 1994). Horizontal section not drawn to scale.

The geochemistry of production well discharge fluids

1. Chemical Composition of the waters

The well discharge fluids based on the relative Cl-SO_4-HCO_3 contents

The classification of fluids is initially attained with the comparison of the relative abundance of the major anions found in geothermal waters namely, Cl^-, HCO_3^- and SO_4^-. Suitable samples for solute geothenncmetry plot close to the chloride apex as shown in Figure 4 for wells TM-1, TM-2 and KN-3. Tlie analytical chloride concentrations reach as high as –14,000 mg/kg with sodium and potassium as major cations. TM-1 and TM-2 have similar chloride concentrations compared to the slightly higher concentrations of KN-3 whch appears affected by boiling at depth. The sulfate concentrations are relatively low for these neutral pH fluids at less than 100 mgkg as analysed compared to other wells in Sandawa which are >300 mg/kg. TM-3 discharge is a mixed sulfate chloride water (inverted triangles in plot), and may have formed through the mixing of acid sulfate waters that have percolated deeply to the depths tapped by the well. The steam trapped at the subzone condense and dilute the rising chloride water. TM-3 produces at –800 masl where a steam cap is beiieved to exist (PNOC-EDC, 1994).

The source of the fluids based on Cl-Li-B contents

Conservative components remain unchanged once added to the fluid (Giggenbach, 1988; Simmons, 1997) and are used to evaluate the origins of the fluid, as well as deduce boiling and dilution processes within reservoirs. The relative proportions of boron and chloride plotted against another conservative component, such as Li, relate to deeper links among the subsystem. The waters discharged by TM-1, TM-2 and KN-3 have a B/Cl ratio of about 4.02 suggesting a common deep source of the fluids. Well KN-3 shows a slight shift consistent with absorption of low B/Cl steam which may mean that there are still magmatic vapors feeding into the system.

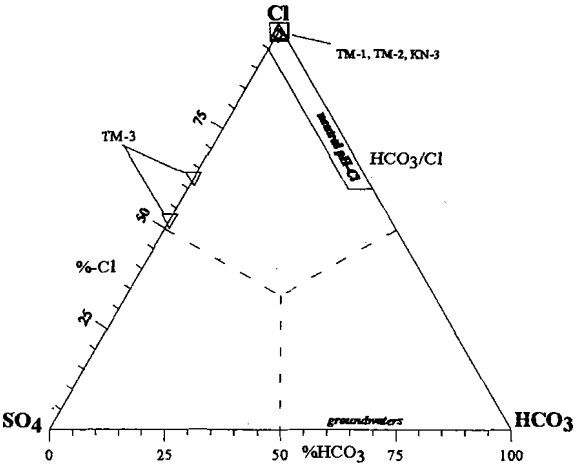

Figure 4. The Cl-HCC3-SO4 diagram. Two types of waters are discharged by the wells, near neutral to neutral pH chloride water and the mixed chloride sulfate water.

Reservoir temperatures

Equilibration conditions can be assessed by the use of the Na-K-Mg diagram. The relationship of these three components is based on temperature dependent exchange of two reactions involving the minerals albite, adularia, illite, chlorite and chalcedony (Giggenbach, 1988). Two geothermometers are derived for the reactions involving the ratios of K/Na and K/Mg. Similar tempemtures indicated by the geothermometers suggest equilibrium conditions. The position of the data points in Figure 8 shows that well waters are in full equilibrium, i.e. $T_{kn} = T_{km}$. The equilibrium temperature indicated is 320°C. The projection of the partially equilibrated or "immature" fluids of TM-3 to the full equilibrium curve suggest a temperature of 260°C. This correlates with the idea that the residual fluids originated from the boiling of the fluids from deeper zones tapped by TM-1 and TM-2.

The predicted temperatures based on aqueous geothermometers are summarized in Table 1. Measured downhole temperatures for each well are also presented. There is close agreement between the temperatures predicted by the geothermometers with respect to the measured temperatures. The alkali geothennometers approximate the hghest measured temperature at less than 10° difference at a range of 300-319°C. The silica geothermometer on the other hand showed similar temperature estimate with respect to well 'I'M-1 only at –280°C which suggests that the well is within liquid saturation based on the discharge enthalpy. In the overall sense, the reservoir temperature is estimated to be around 300°C. The variations in the temperatures may be attributed to the deep processes affecting the fluids during its ascent to the surface such as boiling and dilution.

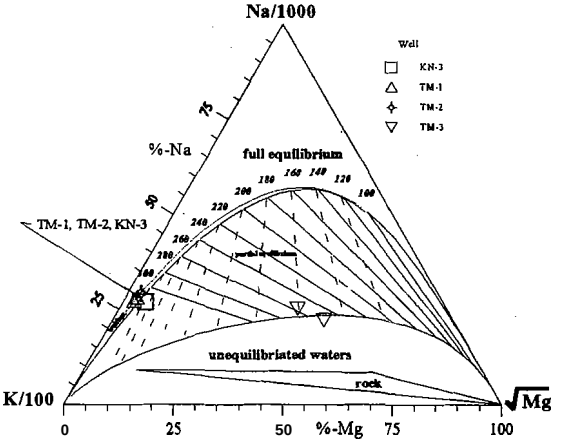

Figure 5. The Na-K-Mg diagram (Giggenbach, 1988). Wells TM-1, TM-2 and KN-3 plot along the full equilibrium line indicating a temperature of 320°C at the reservoir. The projection of TM-3 to the full equilibrium curve shows a temperature of 260°C.

Well	Date	T Qtz [1]	T QA [2]	Na/K [3]	Na/K [4]	Na/K [5]	TNKC [6]	T_{meas} [7]
KN-3	9/1/95	328	316	312	315	319	303	320
TM-1	11/13/95	279	264	315	319	322	301	280
TM-2	4/28/95	288	273	302	301	310	303	272
TM-3	7/29/95	270	259	243	221	257	247	271

Table 1. Aqueous geothermometers based on several authors. TQtz, silica; TQA. quartz adiabatic; TNa/K, sodium-potassium; TNKC, sodium, potassium, calcium.'Fournier and Potter, 1982b; [2]Fournier and Potter, 1982; [3]Fournier, 1983; [4]Truesdell, 1976; [5]Giggenbach, 1983; [6]Fournier and Truesdell, 1983, [7]Downhole measurements taken in 1996 and early 1997 (KN-3 at average)

Chloride-enthalpy relations

The evaluation of boiling and dilution processes affecting the compositions of thermal waters rising to the surface is best exemplified by the chloride-enthalpy plot **(Simmons, 1997).** The enthalpy **of** the corresponding fluid is derived by the **use** of geothermometers or the measured discharge enthalpy of the well. For the plot **shown by** Figure 6, the enthalpy values **are** based on the silica geothermometer which serve as the **best** estimate for reservoir water temperature. The corresponding total discharge chloride concentrations for each well were corrected with respect to the enthalpy based on silica. The intersection of the boiling and dilution lines determines the initial fluid composition. The composition of the initial fluid is projected to be **KN-3** which has the highest Cl content of ~6600 mgkg at **an** enthalpy of **1500** kJ/kg. Well **TM-1** and **TM-2** suggest the fluids are affected **by** dilution.

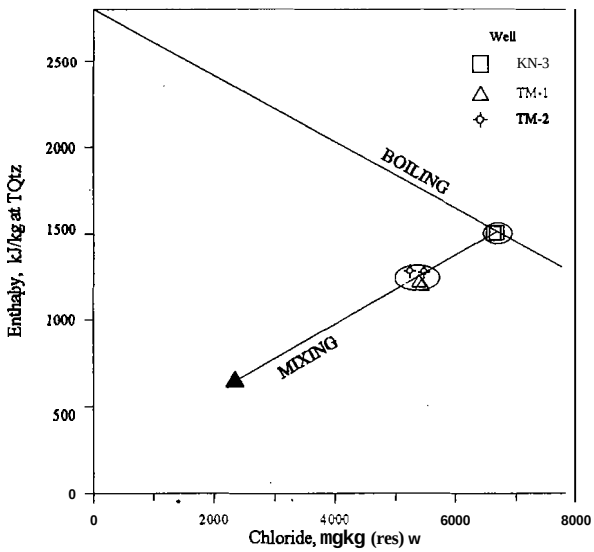

Figure 6. The Cl-enthalpy diagram. The projected parent fluid based on the wells in the study have a chloride content of ~6600 mg/kg. Dilution is the main reservoir process affecting the jluids as shown by TM-1 and TM-2.

2. Evaluation of gas contents of the discharge

The chemical compositions of the gases of the wells selected in **this** *study* are presented in Table **2.** The concentrations are expressed in mmol/mol on *dry* gas basis. The corresponding discharge enthalpy, sampling collection pressure, steam fraction, y_s, and gas fraction, x_g, are **also** shown. The summary of various **gas** geothermometers are shown in Table 3 with corresponding temperatures based on the silica and the sodium, potassium and calcium contents.

The methane and ammonia geothermometers showed lower temperature range estimates at 215-250°C compared to the measured and solute temperatures. However, comparable results are reported by the D'Amore and Panichi (TDAP) and carbon dioxide-argon **(TCA)** geothermometers with respect to the **measured** temperatures. Despite the comparable result given **by** TDAP, it is in contrast with the prescribed reaction. The empirical geothermometer assumes the existence of **free carbon** (graphite) in

the system to react with CO_2 and H_2 to form methane (D'Amore and Panichi, 1980, 1991), however, no carbon mineral occurs found in the wells. Hence, the DAP equilibration temperature appears coincidental. The differences in the predicted temperatures of the gas geothennometers can be attributed to the re-equilibration rates of the gases, reactions with the rack or mixing with deep percolating groundwater.

Well	DATE	H_d	SP	x_g	y_s	CO_2	H_2S	NH_3	H_2	Nz	CH_4
KN-3	9/1/95	1912	0.524	1.47	0.601	915	81.99	0.544	0.391	1.581	0.080
TM-1	11/13/95	1292	0.827	2.29	0.276	934	61.09	0.786	**0.324**	4.023	0.059
TM-2	04/28/95	1728	0.786	1.26	0.492	880	116.45	0.794	0.302	1.997	0.014
TM-3	07/29/96	1251	0.565	1.90	0.282	919	77.08	0.948	1.044	2.159	0.068

Relative N_2-Ar-He contents

The inert gases are used for identifying the deep magmatic source of the fluids. Figure 7 shows that the distribution of the data points for the Sandawa wells falls within an N_2/Ar molar ratio of 70-75. This indicates a basaltic source of the exsolved gases (Giggenbach, 1992) whch is contrary to the fact that the Mt. Apo system is an andesitic system. However, this may be explained by the degassed nature of the fluids in the system. In an earlier version of the N_2-He-Ar plot (Giggenbach, 1992), the Sandawa gases can be defined to be mantle derived with respect to the He isotope.

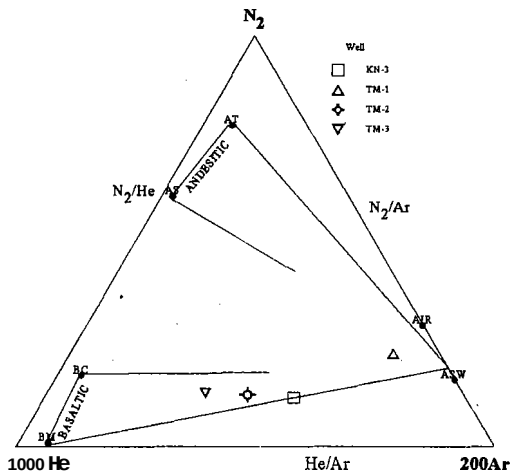

Figure 7. The N_2-He-Ar diagram (Giggenbach, 1992). Exsolved gases from the selected wells suggest basaltic origins. BC, basaltic contaminated; BM, basaltic mantle; AS. andesitic subducted; AT, andesitic thermogenic; ASW, air saturated water.

Total discharge gas distribution

The CO_2 total discharge concentration for the Sandawa wells in this study are generally low at less than 100 mmol/100 mol. The CO_2/H_2S ratios fall between 5-12. As for steam wells, e.g. TM-3, the gas concentrations reach as high as ~350 mmol CO_2/100 mol total discharge. The total discharge gas concentrations are determined from a calculation using the steam fraction at the sampling pressure. The CO_2/H_2S ratio versus the CO_2 total discharge concentration (Figure 8) is useful in determining the steam separation of a particular discharge (Glover, 1970). Gas fractionation curves in single step and multi-step steam separation are modeled assuming an initial gas concentration in the liquid In Figure 8, the curves have been approximated with an initial gas concentration of 300 mmol CO_2/100 mol at 300°C. TM-1 plotted along the residual fluid close to the values at 280°C. Lower gas ratios for KN-3, TM-2 and TM-3 depart from the residual liquid line. This may suggest two-phase conditions at the reservoir. Furthermore, steam fiom TM-3 may be a result of continuous separation of fluids from either KN-3 or TM-2.

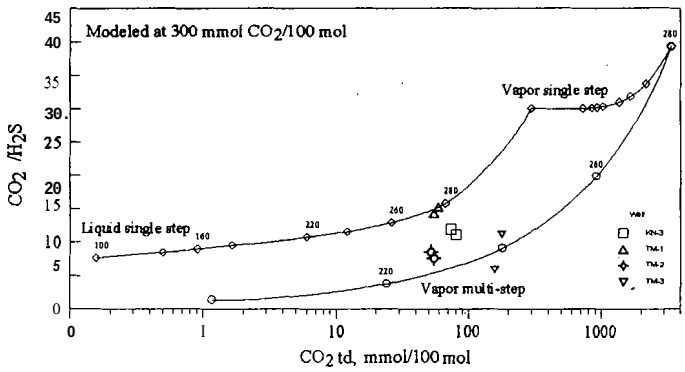

Figure 8. *Gas fractionation diagram modeled at 0.16 m CO_2 initial concentration at* 300°C.

Gas equilibration

Giggenbach (1980) outlined a way of estimating equilibration conditions based on the system H_20-CO_2-H_2S-NH_3-H_2-N_2-CH_4. Initially, the equilibrium constants for methane and ammonia were evaluated. These are based on the reactions,

$$CH_4 + 2H_20 = CO_2 + 4H_2 \quad (1)$$
$$2NH_3 = N_2 + 3H_2 \quad (2)$$

The analytical concentration quotients were evaluated by way of correcting gas contents using the gas distribution coefficients based on an estimated reservoir temperature and a single step model. The new concentration quotients for methane and ammonia are

$$K''_C = X_{d,CO2}\, X^4_{d,H2} / X_{d,CH4}\, (1\text{-}x_g y_s B_{CO2,t})^4 \quad (3)$$
$$K''_N = X_{d,N2}\, X^3_{d,H2} / X^2_{d,NH3}\, (1\text{-}x_g y_s B_{CO2,t})^2 \quad (4)$$

where $X_{d,i}$ are total dscharge gas concentrations corrected for incomplete partitioning of the gases into the steam phase and $B_{CO2,t}$ is the distribution coefficient of CO_2 at the reservoir temperature. The correction is based on the following equation

$$X_{d,i} = x_{s,i}\, x_g\, (1\text{-}y_s + B_{s,i} y_s) / B_{s,i} \quad (5)$$

where x_s is the analytical gas concentration on water free basis, x_g is the total gas content in mmol/mol, y_s is the steam fraction at collection temperature or pressure, and $B_{s,i}$ is the gas distribution coefficient at steam collection.

The log values of K''_C and K''_N based on equations (3) and (4) are plotted against the temperatures derived from the silica and the sodium, potassium and calcium contents as shown in Figure 9 a and b. The diagram shows contours that relate to the effects on K or steam gain ($+y_i$) or loss ($-y_i$) relative to a

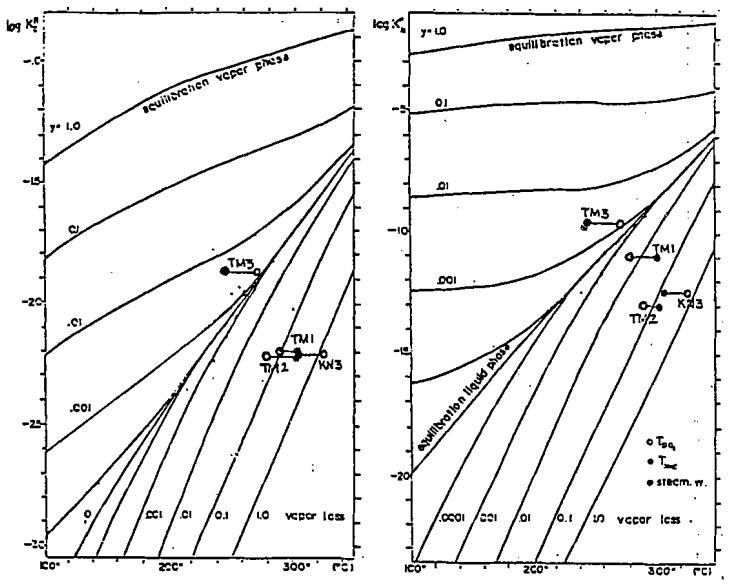

Figure 9 a and b. The log K''_C and log K''_N diagram. Vapor losses are indicated for wells TM-I TM-2 and KN-3.

single phase fluid (y = 0). The gain or loss of vapor is a hypothetical state which represents the composition of the liquid remaining after isothermal evaporation (Giggenbach, 1980). The plots are based on the analyses given in Table 2. The data points for the Sandawa well discharges plot away from the equilibrium liquid phase line indicating vapor losses. The depletion is congruent with the fact that the fluids are indeed degassed. In general, the well discharges in Mt. Apo show low gas concentrations at less than 100 mmol CO_2/100 mol steam. Even the vapor dominated production wells (Salonga, 1994) in Mt. Apo discharge as much as –200 to 350 mmol CO_2/100 mol which are low compared to wells of other geothermal fields. The degassed nature of the Sandawa fluids may have a bearing in the equilibration of the gases in the system. With the disturbed state of gas equilibration, temperatures derived based on the K" values are too low at 216-240°C for $TK"_C$ and 210-253°C for $TK"_N$ (Table 2). However, it gave a higher approximation with respect to the vapor dominated well TM-3 at 262-281°C.

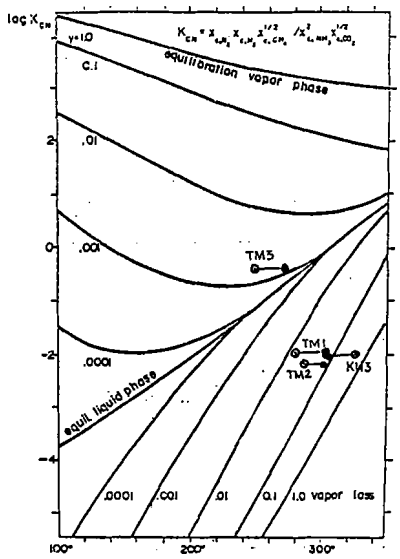

Figure 9c. Log K_{CN} diagram. Vapor losses of up to 5% is implied for the system.

A way of eliminating the dependence of the K" values to the gas or total pressures prevailing in the equilibration zone is attained by combining the relationships (1) and (2) of the two independent systems involving each total gas pressures (Giggenbach, 1980). The total partial pressure for methane is taken to be equal to the total partial pressure of nitrogen which allows the combination of equations (3) and (4) to form a pressure independent relationship given by

$$K_{CN} = X_{c,N2} X_{c,CH4} X^{½}_{c,CH4} / X^{2}_{c,NH3} X^{½}_{c,CO2} \qquad (6)$$

where $X_{c,i}$ is the analytical data of the gas on a water free basis corrected for incomplete partitioning of gas i into the steam phase; the gas fraction, x_g, is not required for the determination. Again the log K_{CN} values are plotted against the temperature as shown in Figure 12c. The data points for the Sandawa well cluster within a small region suggesting vapor loss at an average of –5% whereas the steam discharge of well TM-3 maintains a vapor gain of ~0.1-0.3%. The steam produced signified by TM-3 discharge may be entirely separated steam from the degassed fluids.

Another way of establishing gas equilibration is by the use of the hydrogen-argon (Log HA) and carbon &oxide-argon (Log CA) diagram. Here, the mole ratios of H_2/Ar and CO_2/Ar are plotted (Figure 13). There are two lines shown in the diagram, one representing the composition of the gases in equilibrium with the liquid phase and the other is the equilibration of the gases with the vapor phase. The lines linking the liquid and vapor equilibrium lines correspond to two-phase conditions. With the data reported in Table 2, the Sandawa wells plot below the equilibrium liquid line which suggest unequilibrated gases in the system. Two temperatures can be read off from this diagram to indicate gas equilibrium in the liquid phase; the H_2-Ar temperature ranges 260-270°C and the CO_2-Ar temperature ranges 290-305°C. These Lover the measured temperatures in wells and predicted by solute thermometry. Note that the CO_2-Ar gives higher temperatures which can be representative of the deeper environment. The CO_2 equilibration rate is slow at lower temperatures which may explain the higher temperature estimate.

Fluid –mineral equilibria

Alteration mineralogy reveals several aspects of a system in terms of the type of fluids, temperature, subsurface processes such as boiling and permeability (Browne and Ellis, 1970). The discharge fluid from a well provides a way to evaluate the chemical equilibria and relate this to the minerals found in the altered rocks. This correlation involves the determination of activities of aqueous species calculated to reservoir conditions which follow the principle of thermodynamics, mass balance and chemical equilibria (Ellis, 1977). A program named WATCH for water chemistry was developed by Stefan Arnorsson of the United Nations University, Iceland was utilised to do the chemical speciation. The details on the use of the program are discussed in detail in a paper by Stefan Arnorsson (1981). The computer program is essentially used to calculate the composition and aqueous speciation of geothermal reservoir fluids including pH, redox potential and gas partial pressures given a set of parameters e.g. temperature and enthalpy. It requires analytical compositions of water and gas samples taken simultaneously at a specified sampling pressure. Its application is suited for geochemical data from wet steam wells, hot-water wells and boiling hot springs. In PNOC, the program has been extensively utilized in studies on chemical changes in water chemistry accompanying boiling and cooling in relation to fluid mineral equilibria (e.g. Salonga, 1994).

Well	Temp	pH	logm	log activity			log Q/K	
	°C	res	H_2CO_3	[K]/[H]	[Na]/[H]	$[Ca]/[H]^2$	Ct	Ah
TM-1	280	5.50	-2.07	3.45	4.24	7.21	-0.845	-0.019
TM-2	272	5.76	-3.03	3.72	4.59	7.55	-1.488	0.043
KN-3	320	5.30	-2.68	3.36	4.11	7.10	-1.245	0.455

Table 3. Calculated activities and saturation indices for the Sandawa wells.

the rock cuttings and cores of the wells drilled in the Sandawa Collapse. Here, mineral saturation of anhydnte and calcite are evaluated. The program WATCH determines the analytical equilibrium constant, Q, and is compared with the theoretical i.e. thermodynamically derived, equilibrium constant, K. The quotient expression, Q/K, constitute the saturation index of the mineral. The plot of log Q/K of the

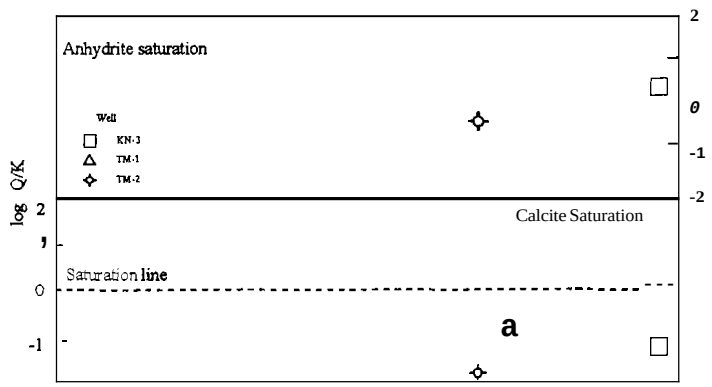

the fluids, TM-1 and KN-3 indicate saturation with respect to anhydrite at reservoir conditions TM-2 appears to be undersaturated but approach saturation at the reservoir. Anhydrite occurs in minor abundance at the reservoir part of well KN-3 and TM-1 and persists in moderate abundance in well TM-2. The deposition of anhydrite can be correlated with respect to the relative abundance of sulfate in the waters. Based on a study by Salonga (1994) wells east of KN-3 (Figure 2) have high sulfate concentrations at >300 mg/kg. It appears that at the sector where the production wells are located, sulfate is reduced in the fluids by the deposition of anhydrite as it migrates westward to the Marbel Corridor. The transition can be attributed mainly to the solubility of anhydrite decreases at lower temperatures.

The discharge fluids of the wells are all undersaturated with respect to calcite at the reservoir which can be attribute to the slightly acidic condition of the reservoir fluids. Calcite prefers to be dissolved in acidic media, however, calcite is observed to be present at the shallow zones in these wells at about ~1200-1500 masl in greater abundance as open-space fills which may reflect boiling conditions.

Mineral stability

The equilibrium states of the Na^+, K^+ and Ca^{++} mineral species are also evaluated through the use of the mineral stability diagrams. The mineral stability diagram is a plot of activity quotients involving Na^+, K^+, Ca^{++} and H^+ at a calculated temperature. The basis for such relationship lies in the mineral reactions involving the ion species. The detail on the use and construction of mineral stability diagrams are discussed by Browne and Ellis (1970).

In Figure 11, the Na_2O-K_2O-Al_2O_3-SiO_2-H_2O system shows the mineral stability boundaries at 300 and 280°C. This system shows how aqueous Na^+, K^+, H^+ and SiO_2 relate at equilibrium conditions to albite, kaolinite, K-mica (illite or muscovite), K-feldspar (adularia) and quartz. Based on the positions of TM-1, TM-2 and KN-3, the reservoir liquid is in equilibrium with K-mica at 300 and 280°C. Well TM-2 composition plots close to the stability boundary where albite, K-feldspar and K-mica coexist. This means that if Na^+ and K^+ will be fixed in the mineral phase, albite, adularia or illite will form. Illite is extensively found below sea level in the wells drilled where temperatures reach 300°C; adularia on the other hand was found only in well KN-3.

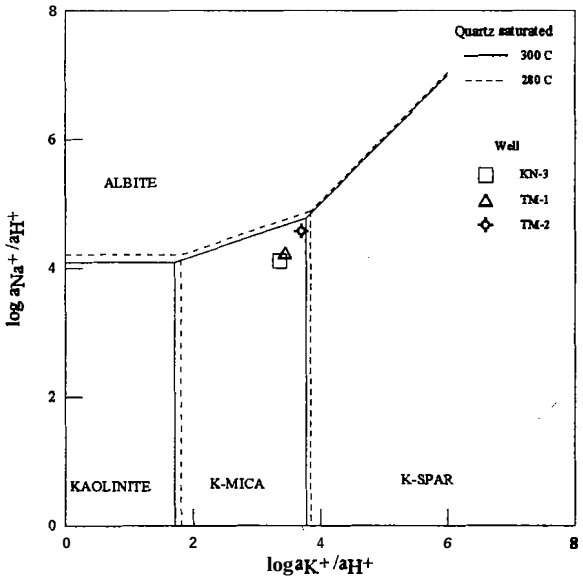

Figure 11. The Na_2O-K_2O-Al_2O3-SiO_2-H_2O mineral stability diagram, TM-I, TM-2 and KN-3 fluids are in equilibrium with K-mica at 300°C and 280°C. TM-2 fluids approach equilibrium with albite, adularia and k-mica.

The composition of the waters are also plotted in the CaO-K_2O-Al_2O_3-SiO_2-H_2O±CO_2 system (Figure 12) which shows how aqueous Ca^{++}, K^+, H^+ and SiO_2 relates to the stability of mineral phases. In Figure 12, the mineral stability boundaries at 300°C and 280°C are shown. Note that the 280°C boundary line is already coincident with 300°C. The horizontal dashed lines represent the value at which calcite will replace other calcium silicates, e.g. wairakite depending on the concentration of dissolved CO_2 in the fluids (Browne and Ellis, 1970). The aqueous compositions of TM-1 and KN-3 are in equilibrium with wairakite, K-mica (illite) and calcite at reservoir conditions. Well TM-2 is in equilibrium with wairakite, K-mica, K-feldspar (adularia) and calcite. Calcite, wairakite, illite, epidote, are found in TM-1 and TM-2; illite, calcite, epidote and adularia are found in KN-3 based on the rock cuttings. In retrospect, the existing fluids may be a derivative of boiled and diluted fluids which allowed the formation of the minerals. Initially, the fluids are in equilibrium with K-mica; loss of steam increases the pH and the water cools' shifts the

(Browne and Ellis, 1970). Calcite continues to precipitate as CO_2 is lost to steam.

Hydrogen-hydrogen sulfide equilibria

Hydrogen sulfide is one of the dominant gases found in geothermal fluid discharges. The partial pressures of H_2S and H_2 are used to relate to the stabilities of sulfide mineral species, more particularly pyrite and pyrrhotite and an Fe-bearing alumino-silicate such as chlorite or epidote. Giggenbach (1980) derived three equilibrium constants relating the gas concentrations of H_2S and H_2 based on the reactions,

$$FeS_2 + H_2 = FeS + H_2S \quad (7)$$

$$3FeS_2 + 2H_2 + 4H_2O = Fe_3O_4 + 6H_2S \quad (8)$$

$$FeS_2 + H_2 + (H_2O) = (FeO) + 2H_2S \quad (9)$$

and the equilibrium constants corrected for incomplete partitioning are the following equations,

$$K'_{PP} = X_{c,H2} / X_{c,H2S} \text{ (py- pyrrhotite)} \quad (10)$$

$$K'_{CM} = X^6_{c,H2S} X_{c,CH4} / X^6_{c,H2} X_{c,CO2} \quad (11)$$

(pynte-magneutte)

$$K'_{CA} = X^2_{c,H2S} X^{1/4}_{c,CH4} / X^2_{c,H2} X^{1/4}_{c,CO2} \quad (12)$$

(pyrite-Fe-Al-silicate)

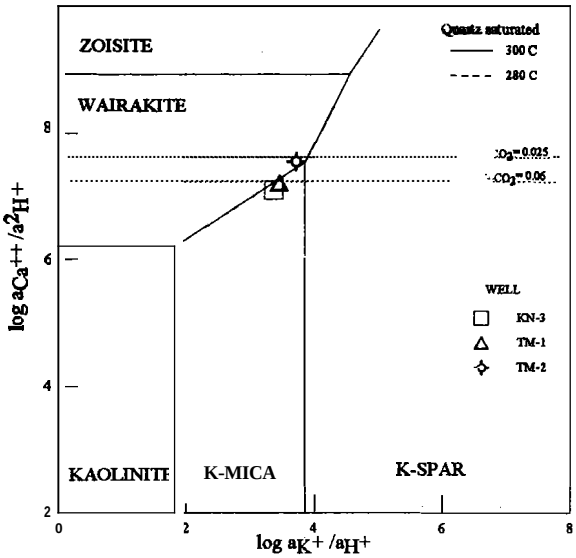

Figure 12. The $CaO-K_2O-Al_2O_3-SiO_2-H_2O\pm CO_2$ mineral stability diagram. Epidote is treated as zoisite. Horizontal lines indicate molal concentrations of carbon dioxide in the liquid.

where Xc are the analytical data corrected for incomplete partitioning earlier described. The equations are again rewritten in terms of $S = X_{c,H2} / X_{c,H2S}$ and $C = X_{c,CH4} / X_{c,CO2}$, thus

$$\log S_{PP} = -\log K'_{PP} \quad (13)$$

$$\log S_{CM} = (\log C)/6 - (\log K'_{CM})/6 \quad (14)$$

$$\log S_{CA} = (\log C)/8 - (\log K'_{CA})/2 \quad (15)$$

The results of log S are plotted against silica and Na-K-Ca temperatures in Figure 13. The data plot show well within the pyrite stability field suggesting that H_2/H_2S ratios are externally controlled. The other sulfur species that may have influenced the equilibria is sulfate (Giggenbach, 1980). Salonga (1995) pointed out that the solubilities of Fe* and Cu are influenced by redox state and the pH level of the fluids. The presence of sulfate-rich fluids at the eastern sector of Sandawa Collapse could be an influencing factor in the composition of the fluids. It seems that the H_2S is consumed i.e. oxidized rather than produced from the reaction of these sulfide minerals. Sulfur isotope studies on Mt. Apo indicate that H_2S in the fluids are derived from a magmatic source (Bayon, 1995). H_2S is oxidized at boiling depths to form sulfate which percolate into deeper horizons.

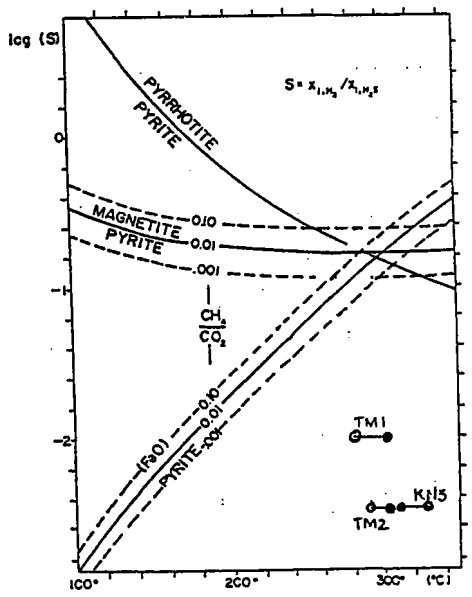

Figure 13. Log S to assess variations in H_2/H_2S ratios affecting sulfide mineral stability.

Conclusions

The wells in the study namely, TM-1, TM-2, TM-3 and KN-3, demonstrate a small aspect of the overall geochemical structure of the Mt. Apo system. These wells among others (e.g. KN-1, KN-2, PS-I) were drilled within the Sandawa Collapse which is believed to be the hottest part of the system. The geothermal waters upflow from this area and migrate northwest into the sector named the Marbel Corridor (Figure 3).

Well KN-3 is the deepest well drilled within the sector, the other wells were drilled southwest of KN-3. Hydrothermal minerals found in the wells consist mainly of the temperature dependent spectrum illite + epidote + actinolite + secondary biotite and chlorite + quartz + calcite + anhydrite + pyrite which is the common assemblage in a dominantly neutral pH environment. Based on this assemblage, there is a progressive temperature increase with respect to depth reaching 300°C. Measured downhole temperatures indicate a range of 272-328°C (Table 1) at reservoir depths below 800 masl.

The waters discharged by the wells are characterized to be near neutral to neutral pH chloride and mixed chloride sulfate waters (Figure 4). The chloride waters comprise the fluid at the reservoir. The mixed chloride sulfate waters are believed to have formed at the shallower horizons of the system (~500-800 masl) brought about by mixing of deeply percolating acid sulfate waters from the surface with the rising chloride waters diluted by condensing steam tapped by well TM-3. Deep temperatures assessed through aqueous geothermometers vary from 270 to 320°C are consistent with the predicted temperatures from mineral geothermometry and measured downhole temperatures. Equilibration temperatures depicted by the Na-K-Mg dagram (Figure 8) show fully equilibrated waters tapped by the wells (TM-1, TM-2, KN-3) indicating a temperature of 320°C. The projected parent fluid have a Cl content ~6600 mg/kg (Figure 6) represented by the waters tapped by KN-3. Dilution or mixing appears to be the main process affecting the fluids as it rises to shallower horizons of the reservoir as evidenced by the lower chloride content of well TM-1 and TM-2. However, discharge characteristics suggest two-phase conditions (Figure 8) where discharge enthalpies are greater than the enthalpies based on silica and cation geothermometers.

Gas discharges of the wells indicate that the fluids have undergone continuous degassing (Salonga, 1994) during the ascent from deeper horizons to the present reservoir depths tapped by the wells. The degassing is presently occurring as shown by the two-phase conditions exhibited by the well discharges. Gas contents of the fluids are low which vary from 60-80 mmol CO_2/100 mol and 4.5-6 mmol H_2S/100 mol. The degassed characteristics of the fluids are reflected in gas equilibration resulting to vapor losses in TM-1, TM-2 and KN-3 to as much as 5% (Figure 9 a, b, c). The vapor gain in TM-3 may be a result of steam separation from the fluids of TM-1, TM-2 and KN-3. The gases are also assessed to be unequilibrated based on the CO_2/Ar and H_2/Ar ratios. Gas geothennometers predicted a variable range of temperatures from 210-321°C, however, the temperatures estimated by the carbon dioxide-argon geothermometer are in accord with measured downhole temperatures.

Aqueous speciation of the discharge fluids fiom the wells (TM-1, TM-2, KN-3) indicate saturation with respect to anhydrite and undersaturation with calcite at reservoir conditions (Figure 10). However, both these minerals are found in the rock cuttings of the wells, probably as a result of the continuous degassing of the fluids. With respect to the cationic components, the fluids are found to be in equilibrium with K-mica at the reservoir (Figure 11, 12). Moreover, conditions for well TM-2 indicate that the fluids are also in equilibrium with albite, wairakite, K-feldspar and calcite. Owing to the low CO_2 content of the fluids, the calc-silicates may form readily. Hydrothermal alteration mineralogy from these wells indicate wairakite, adularia and calcite are found to exist in these conditions.

Furthermore, hydrogen-hydrogen sulfide equilibria are not controlled by the reactions involving sulfides found in the Mt. Apo system, instead they appear influenced by the redox state.

References

Arnorsson, S. and Sigurdsson, S., 1982. The chemistry of geothermal waters in Iceland I. Calculation of aqueous speciation from 0°C to 370 °C. Geochim. Cosmochim. Acta, 46, 1513-1532.

Bayon, F.E.B., 1995. Sulphur isotope applications in two Philippine geothermal systems. University of Auckland Geothermal Institute Project.

Browne, P.R.L., 1997. Lecture notes on geology, hydrothermal alteration and geothermal systems. Geothermal Institute, University of Auckland, New Zealand

Camit, R.A., 1994. Geology of Well KN-3. PNOC Internal Report.

D'Amore, F., 1991. Gas geochemistry as a link between geothermal exploration and exploitation. Applications of Geochemistry in Geothermal Reservoir Development. UNITAR. Co-ordinator: D'Amore, F., pp. 93-108.

Delfin, F.G. and Castro, C.C., 1984. Mt. Apo geothermal project- first stage exploration evaluation. PNOC-EDC Internal Report.

Ellis, A. J. and Mahon, W. A. J., 1977. Chemistry and Geothermal Systems. Academic Press. pp. 100-113, 126-133, 144-150, 176-188.

Fournier, R.O. and Truesdell, A.H., 1973. An empirical Na-K-Ca geothermometer for natural waters. Geochimica et Cosmochimica Acta, v. 37, pp. 1255-1275.

Fournier, R.O. and Potter, R.W. II, 1982. A revised and expanded silica (quartz) geothermometer: Geothermal Resources Council Bulletin, November: 3-12.

Fournier, R.O. 1991. Water geothermometers applied to geothermal energy. Applications of Geochemistry in Geothermal Reservoir Development. UNITAR. Co-ordinator: D'Amore, F., pp. 37-66.

Giggenbach, W.F., 1980. Geothermal gas equilibria. Geochimica et Cosmochimica Acta, v.44, p. 2021-2032.

Giggenbach, W.F. and Goguel, R. 1988. Collection and analysis of geothermal and volcanic water and gas discharges: DSIR Chemistry Division Report No. CD 2401, fourth edition.

Giggenbach, W.F., 1991. Chemical techniques in geothermal exploration. Applications of Geochemistry in Geothermal Reservoir Development. UNITAR UNDP. Co-ordinator: D'Amore, F., pp. 93-108.

Giggenbach, W.F., 1992. The composition of gases in geothermal and volcanic systems as a function of tectonic setting: Water-Rock Interaction-7 (ed. Y.K. Kharaka & A.S. Maest), vol. 2, p. 873-878.

Glover, R.B., 1970. Interpretation of gas compositions from the Wairakei field over 10 years. U.N. Symposium on the Development and Utilization of Geothermal Resources. Geothermics (1970)- special issue, pp. 1355-1366.

Hedenquist, J.W., 1990. The thermal and geochemical structure of the Broadlands-Ohaaki geothermal system, New Zealand Geothermics, Vol. 19, No.2, pp. 151-185.

Henley, R.W., Truesdell, A.H. and Barton, P.B. Jr., 1984. Fluid-mineral equilibria in hydrothermal systems. Reviews in Economic Geology, Vol. 1. Ed: J.M. Robertson, Society of Economic Geologists. vol. 1, 267 pp.

Maturgo, O.O. and Zaide-Delfin, M.C., 1993. Geology of well KN-1D. PNOC Internal Report

Maturgo, O.O. and Rosell, **J.B. 1993.** Geology **of** well KN-2D. PNOC Internal Report.

Maturgo, O.O., **1995.** Chemical characteristics of acid fluids in some PNOC geothermal wells. PNOC Internal Report. Presented in the **1995** PNOC Geothermal Conference, Manila, Phlippines.

Panem.C.C., **1995.** Geology of well TM-3D. PNOC Internal Report.

Ping, Z., **1991.** Gas geothermometry and chemical equilibria of fluids from selected geothermal fields. UNU Geothermal Training Project.

Rosell, J.B., **1994.** Petrology of well KN-3. PNOC Internal Report.

Rosell, **J.B., 1994.** Petrology **of** well TM-1D. PNOC Internal Report.

Rosell, J.B., **1994.** Petrology of well TM-2D. PNOC Internal Report.

Salonga, N.D., **1995.** Fluid and mineral equilibria in acid NaCl(+SO4) reservoir: The case of Sandawa Collapse, Mt. Apo Hydrothermal system. PNOC Internal Report.

Sambrano, B.G., **1994.** Geology of well TM-1D. PNOC Internal Report

Sambrano, **B.G., 1994.** Geology of well TM-2D. PNOC Internal Report

Simmons, S.F., **1997.** Lecture notes on geochemistry and geothermal systems. Geothermal Institute, University of Auckland, New Zealand.

_____, **1989.** Mt. Apo Geothermal Project: Preliminary resource assessment. PNOC-EDC Internal Report.

_____, **1994.** Mindanao 1 Geothermal Project. resource assessment Update. PNOC-EDC Internal Report.